JOURNAL OF MATERIALS SCIENCE 35 (2000) 5263–5273

The erosive wear of mild and stainless steels under controlled corrosion in alkaline slurries containing alumina particles

H. W. WANG*, M. M. STACK
Corrosion and Protection Centre, University of Manchester Institute of Science and Technology, PO Box 88, Manchester M60 1QD, UK
E-mail: hong.w.wang@umist.ac.uk

The erosive wear in an alkaline slurry containing alumina particles of three typical engineering materials, the mild steel BS 6323 (Fe-C), the AISI 410 stainless steel (Fe-Cr-C), and the AISI 304 stainless steel (Fe-Cr-Ni), was carried out, by means of rotating cylinder, three-electrode erosion-corrosion test, with a view to investigation into the roles of the typical elements and the mechanical and chemical properties in the erosive wear under simultaneous controlled corrosion. The total weight loss of erosion-corrosion was obtained by precision weighing and the result was compared and interpreted, for each material, by a full microscopical examination of the erosion-corrosion scars using scanning electron microscopy (SEM). It was found that the overall performance under erosion-corrosion in an descending order was the stainless steels AISI 304, AISI 410, and the mild steel, although the precise difference in performance was dependent upon the process conditions. Such a ranking of performance was not in total consistence with that expected only from the mechanical or the chemical property differences of the materials concerned. The individual contribution of each erosion and corrosion process was thus further separated through corrosion charge conversion using the Faraday's second law and the results were interpreted by discussion, on basis of the experimental and microscopical evidences, of the main factors that influenced the mechanical and wear behaviour, in conjunction with those influencing corrosion and passivity. Finally, schematic diagrams were proposed to outline the typical erosion and corrosion features thus obtained for all the three materials during erosion-corrosion.

1. Introduction

Erosion-corrosion is a combined mechanism by which materials suffer damage due to erosion and corrosion. Erosion can take the form of either dry solid-particle erosion, resulting from impingement by air-borne solid particles, or wet erosion, due to impact by a rapidly flowing liquid or solid particles entrained in a liquid flow. Corrosion can occur in the form of either dry, high temperature oxidation (hot corrosion) or wet corrosion in (such as aqueous corrosion) or associated with (such as atmospheric corrosion) liquid solutions. Apparently, resistance to both erosion and corrosion is generally required in conditions when any combination of the above erosion and corrosion is involved. However, the overall erosion-corrosion weight loss is usually greater than the sum of pure erosion (free of corrosion) and pure corrosion (free of erosion), associated with an "additive", erosion-enhanced corrosion effect and a "synergistic", corrosion-induced erosion effect [1, 2]. Consequently, the erosion and corrosion, under their mutual influences, essentially differ from the pure erosion and corrosion, respectively, and the influences of variables, pertinent to pure erosion or corrosion, such as the velocity and angle, size, angularity of impact particles [3–7] and the chemical composition, electrochemical nobility, and ability to passivate and stability of the passive film [8–11] could be more pronounced in erosion-corrosion.

Since the contribution of each of such modified erosion and corrosion process determines the overall erosion-corrosion weight loss, it is of both practical importance and theoretical interest to assess the exact role of these two processes and to subsequently control them. The present paper concerns an investigation of three engineering materials of typical compositions, microstructures, and properties, i.e., ferritic-pearlitic mild steel BS6323 (Fe-C), martensitic AISI 410 stainless steel (Fe-Cr-C) and austenitic AISI 304 stainless steel (Fe-Cr-Ni), under erosion-corrosion conditions in an alkaline slurries containing alumina particles, with a view to investigation into the role of mechanical and chemical properties in resisting erosion and corrosion,

* Author to whom all correspondence should be addressed.

and to further assessment of the exact contribution of erosion and corrosion to the overall erosion-corrosion weight loss. This is attempted by controlled erosion (achieved by varying sample rotation speed in a given slurry pot) and controlled corrosion (achieved by potentiodynamic sweeping of the rotating sample in this case), enabling the instantaneous response of the sample corrosion current to be recorded as a function of the potential sweep time, on basis of which the precise corrosion weight loss can be quantified using Faraday's second law. This allows then quantification of the erosion in the overall erosion-corrosion. The justification of the respective role of erosion and corrosion, as compared with each other, will also be addressed and the main erosion-corrosion mechanisms involved, in terms of the particle velocity regimes within which erosion or corrosion dominates, proposed.

2. Experimental details

The erosion of the mild steel, BS6323, AISI 304 stainless steel, and AISI 410 stainless steel was studied, and compared, by means of solid particle erosion under simultaneous corrosion, by potentiodynamic polarisation, in a turbulent alkaline slurry. The test apparatus was a modified rotating cylinder three-electrode (RCE) erosion-corrosion system [12, 13]. Here, Fig. 1 shows further a close-up of the test cell. The RCE rig consists of a hollow cylindrical, working electrode (specimen ring), an auxiliary, counter electrode (platinum foils), both contained in the electrolyte cell, and an outside standard reference electrode (saturated calomel electrode, SCE), connected to the solution by salt-bridging. Electrical connection to the cell, made through the three electrodes, was controlled by an intermediate potentiostat (ACM Instruments). Control signals input to and data acquisition from the potentiostat were made by a computer via a high velocity digital-to-analogue (D/A) and analogue-to-digital (A/D) conversion interface board (Keithley DAS1600), interfaced by an Easyest LX software (Keithley version 3.0). The use of the computer allows playback of programmed tests and thus offers better control of potential than sweep generator.

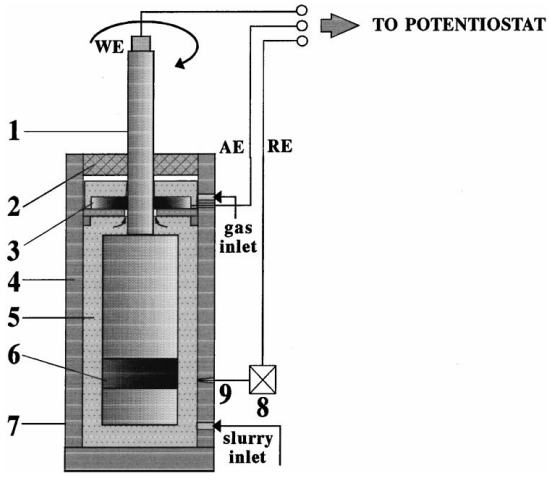

Figure 1 A close-up of the rotating cylinder, three-electrode erosion-corrosion test rig.

TABLE I The composition (main alloying elements), microstructure, and tensile strength of the mild steel, BS 6323, AISI 410 and AISI 304 stainless steels

	Composition (wt%) (main alloying elements)	Microstructure	Tensile Strength (MPa)
Mild steel BS 6323	0.20 C 0.6-1.0 Mn	ferrite + pearlite	450
AISI 410 Stainless Steel	0.12 C 12 Cr	martensite	780
AISI 304 Stainless Steel	0.04 C 20 Cr, 8 Ni	austenite	610

Ring samples, made from wrought, seamless tubes of the selected steels, were machined and polished to a final dimension of 38 mm (outer diameter) by 2–4 mm (wall thickness) by 10 mm (height), appropriately cleaned, dried, and weighed (to an accuracy ± 0.01 mg, using a precision balance, Satorious 2024MP) prior to and after each erosion-corrosion test. Table I shows the typical composition, microstructure, and mechanical properties of the steels. The slurry was an 0.5 M mixed solution, 1 : 1 by volume, of $NaHCO_3$ and Na_2CO_3, prepared out of de-ionised water and sufficiently deaerated using pressurised nitrogen, which contained 150-μm alumina particles of nominal concentrations of 300 g/1000 ml. *In situ* purging of nitrogen into the cell was made during the wear test to maintain the oxygen-free situation, through an upper inlet to the cell which can avoid possible cavitation erosion associated with nitrogen bubbling via a lower inlet. Linear polarisation was conducted from -1.0 to $+1.25$ V at a potential ramp of 2.5 mV/s, with a constant specimen rotation velocity up to 4000 rpm (8 m/s, the equivalent linear speed at specimen surfaces). The rotation of the specimen shaft was stopped when the potential sweep was finished. The response of potentials and electrical currents of the specimen was directly monitored and measured against the running time. The specimen surface after test was characterised mainly by means of scanning electron microscopy (SEM, ISI DS 130).

3. Results

Before particle erosion was introduced, i.e., with the sample being stationary, the sample's corrosion current response to the applied potential sweep described above was obtained in Fig. 2. Such polarisation curves were in contrast to those obtained when particle erosion was introduced at rotating speed of 2–8 m/s (Fig. 3). The weight loss after such tests was determined by weighing, the results are presented as the total erosion-corrosion weight loss as a function of particle speed in Fig. 4. To explain the weight loss differences, post-erosion-corrosion morphological examination of the samples' surfaces was made by means of SEM for evidences of wear and corrosion and their possible mechanisms, shown in Figs 5–7. The coulombic charges due to corrosion, obtained on basis of the polarisation curves of Figs 2–3, for each test were finally converted to corrosion weight loss (Fig. 8a) using Faraday's second law. Subtracting these values from those of Fig. 4 at

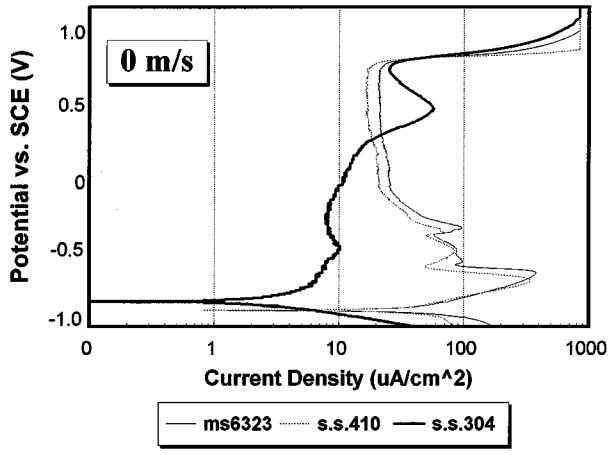

Figure 2 Responses of stationary samples of the mild steel, BS6323, and stainless steels AISI 410 and 304, to anodic, potentiodynamic polarisation in 0.5 M sodium carbonate/bicarbonate solutions containing alumina particles of 150 μm in size, at a sweep rate of 2.5 mV/s from -1 to $+1.25$ V.

corresponding velocities, the erosion weight loss was obtained for all the three materials (Fig. 8b). Comparison of Fig. 8a and b will determine whether erosion or corrosion dominates the overall erosion-corrosion, as to be discussed below.

4. Discussion

4.1. Influences of erosion on the response of corrosion current to applied potential

When the response of the corrosion current to applied potential is free of the influences of particle erosion (Fig. 2), a number of basic corrosion events are identified. Following cathodic evolution of hydrogen, active dissolution and passivation are revealed, and transpassivation occurred above ~0.83 V for all the three materials. However, differences in the corrosion potential, E_{corr}, critical passivation current, i_c, and passivation current, i_p, are clear among them. The value of i_c is ~400 μA/cm^2 for the mild steel, higher than that for the 410 steel (~310 μA/cm^2). This is associated with the higher ability of the latter to passivate by the added ~12% Cr. For the same reason, the value of i_p of the 410 steel (~20 μA/cm^2) is lower than that of the mild steel (~30 μA/cm^2). The high Cr content (with addition of Ni and reduction of C) of the 304 steel (Fe-18Cr-8Ni) confers to it additional passivation capacity (lower i_c) and higher passivation stability (lower i_p), the i_c being ~10 μA/cm^2 in this case, lower than typical values in sulphuric acids [14]. There is no significant difference in the E_p of the three steels, indicating that they all start to form similar passive films (either Fe or Cr oxides) at the initial passivation stage. Peaks at later stages are related to the formation of passive films of increased valence states of Cr or Fe. For example, the peak between 0.4 V and 0.83 V for the 304 steel is due to the conversion of insoluble chromium oxides (Cr_2O_3) into soluble chromate anions (CrO_4^{2-}) (depassivation) and the formation of high-valence iron oxides (re-passivation)[15–17].

A significant influence of the particle erosion on corrosion is seen for the mild and 410 steel (Fig. 3), since not only the active dissolution and critical passivation

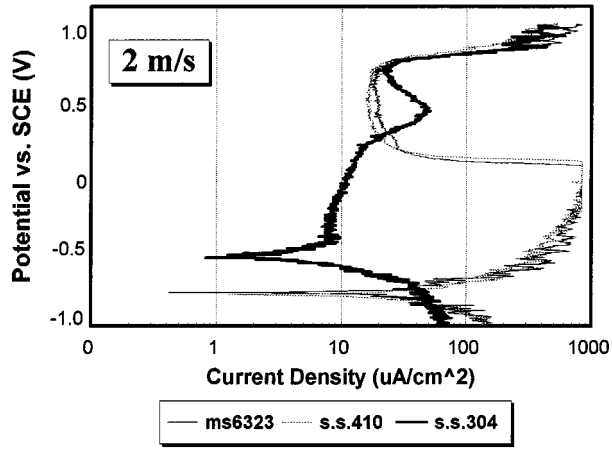

(a)

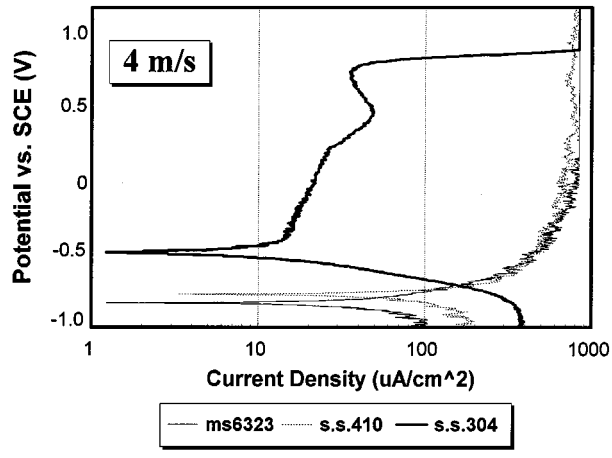

(b)

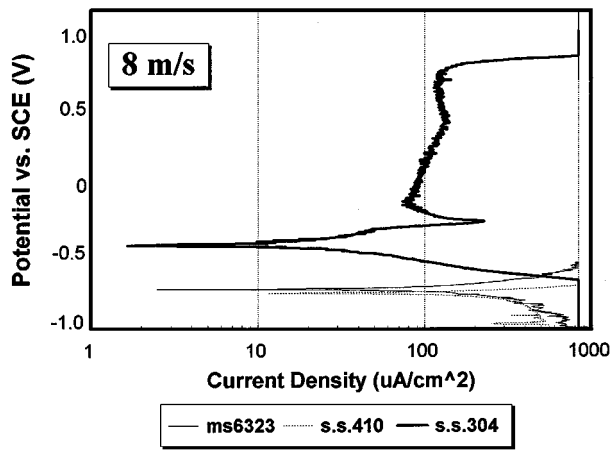

(c)

Figure 3 Responses of rotating samples of the mild and stainless steel to potentiodynamic polarisation of Fig. 2 at a speed of (a) 2 m/s (1000 rpm), (b) 4 m/s (2000 rpm), and (c) 8 m/s (4000 rpm).

current, if any, are greatly increased, but also the passivation region are either reduced (Fig. 3a) or completely suppressed (Fig. 3b). On the contrary, the 304 steel can passivate in the whole speed range, owing to its higher Cr content, though the passivation becomes increasingly difficult (indicated by the increase of E_p) (Fig. 3c). The increased dissolution of Fe or Cr is associated with not only the increased migration and transport of corroding species (anions and cations), due to mechanical stirring, convection, and thermal current [18], but also the "erosion" and disturbance of the established

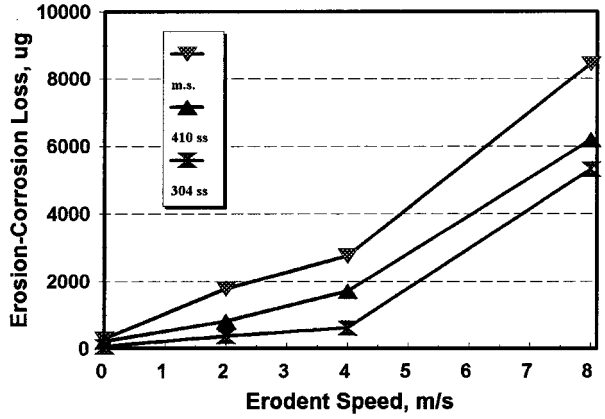

Figure 4 The overall erosion-corrosion weight loss of the mild steel, and stainless steels of AISI 410 and AISI 304, as a function of the slurry speed.

electrochemical double layer (EDL) which would otherwise reach an equilibrium after a certain amount of dissolution is achieved. Since formation of a passive film requires certain amount of metals to be dissolved into the EDL, the competition between the amount of Fe and Cr dissolving into EDL and the amount taken away from EDL due to mechanical removal determines whether or not passivation would be possible at yet higher potentials. This explains the recovery of passivation of the mild steel (also 410 steel) at 2 m/s (Fig. 3) only at higher potentials but at the expense of much higher dissolution at lower potentials. Further, the ability of a damaged passive film to *reheal*, during intervals of two successive particle impacts, is also critical in determining whether a new passive film can still form. This might be the case of the 304 steel which

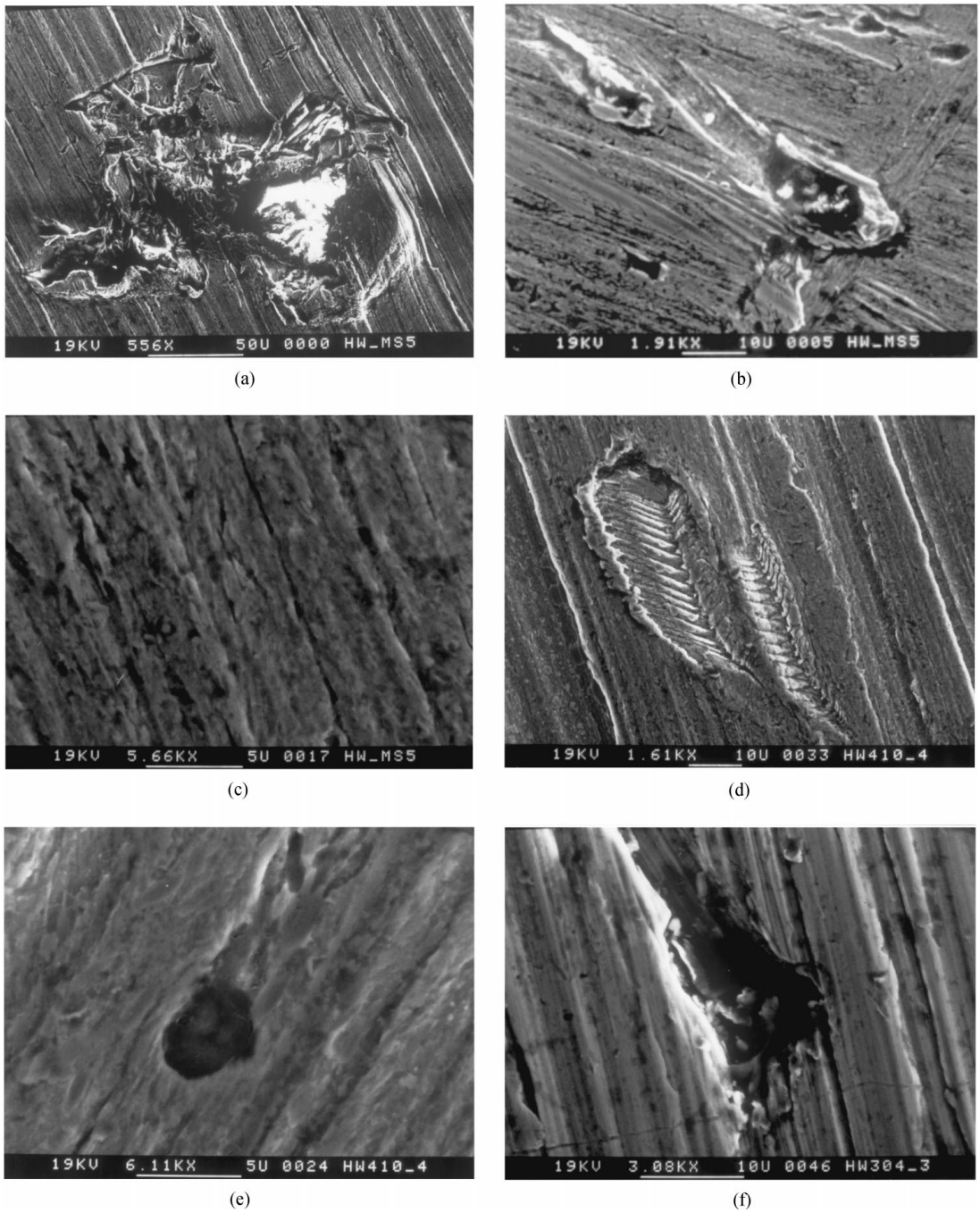

Figure 5 The SEM surface morphology of the mild steel (a-c), the AISI 410 (d,e), and the AISI 304 (f) stainless steels after erosive wear at a slurry speed of 2 m/s (see text for details).

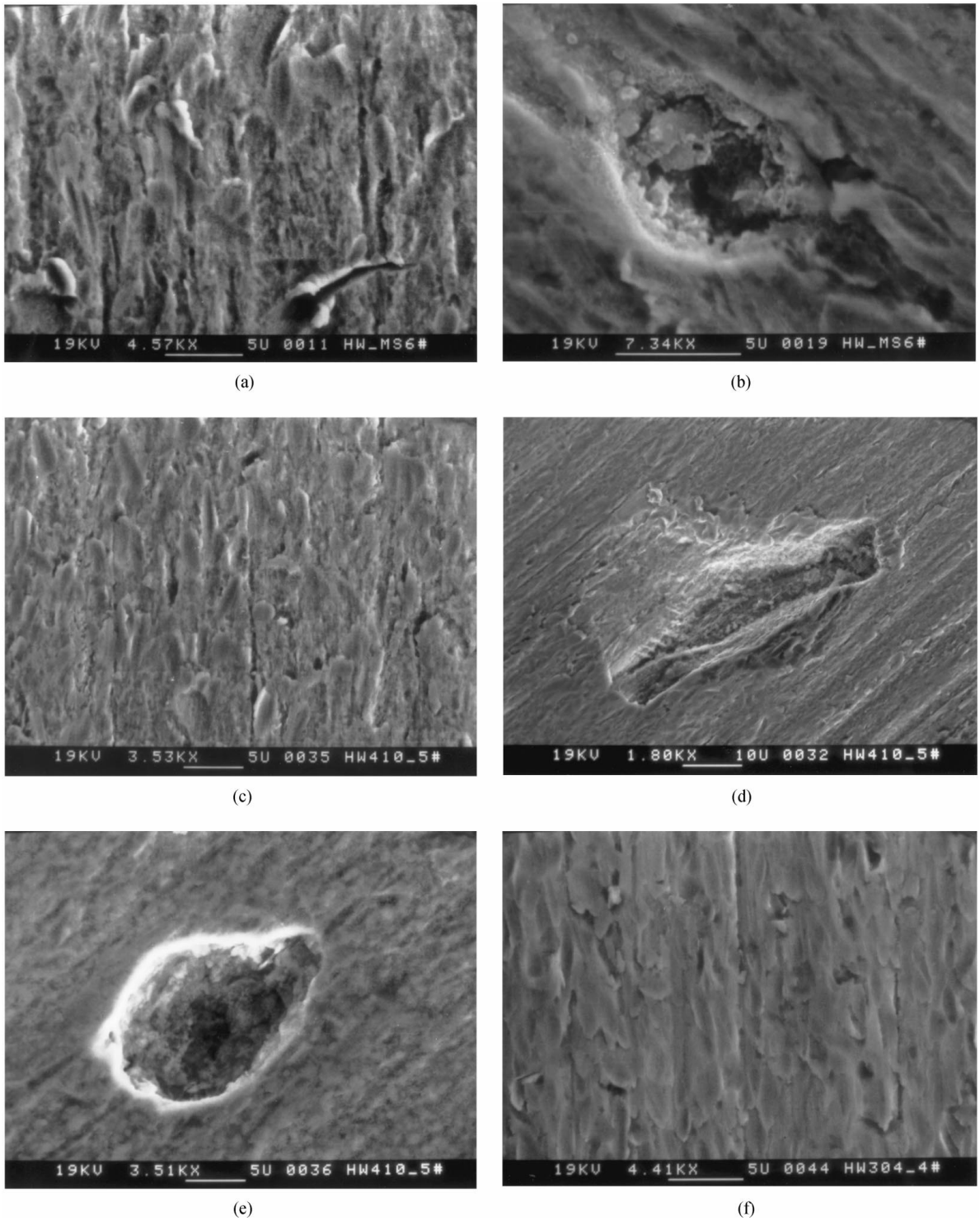

Figure 6 The SEM surface morphology of the mild steel (a,b), the AISI 410 (c-e), and the AISI 304 (f) stainless steels after erosive wear at a slurry speed of 4 m/s (see text for details).

maintains full passivation at all speeds. The damaging effect of erosion (mechanical removal) is more pronounced than that of enhanced corrosion due to increase in mass transfer because erosion is strongly dependent upon the particle kinetic energy or speed while mass transfer is determined by the solution concentration and temperature. This explains why the passivation of the mild and 410 steel (Fig. 3a) could still occur after sufficient amount of elements is dissolved at lower slurry speeds but could not at higher speeds (Fig. 3b and c). The vertical line at $\sim$840 μA/cm^2 indicates the maximum current density that can be conducted for the given solution. The marginal differences in the corrosion performance of the 410 and mild steel (Fig. 2) is reduced as erosion starts.

4.2. The total erosion-corrosion weight loss

The total weight loss (W_{ec}) (Fig. 4), consisting of two components, the erosion weight loss (W_e) and corrosion weight loss (W_c), increases with the slurry speed. Therefore erosion and corrosion both contribute to the overall weight loss. Erosive wear loss generally increases strongly with the particle speed (in a power law

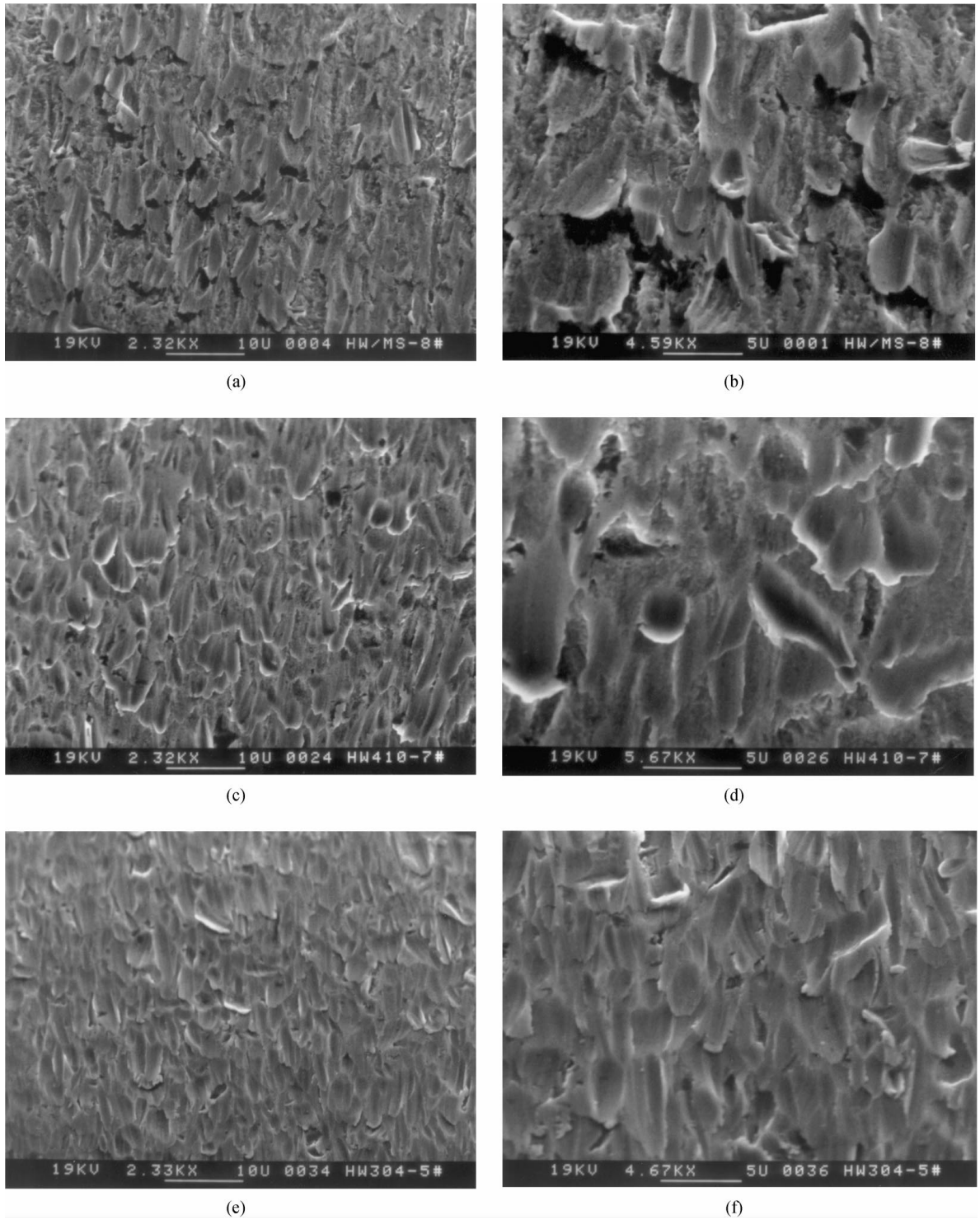

Figure 7 The SEM surface morphology of the mild steel (a,b), the AISI 410 (c,d), and the AISI 304 (e, f) stainless steels after erosive wear at a slurry speed of 8 m/s (see text for details).

relationship for dry erosion). In slurry wear, this increase is due to more intensive erodent microcutting or microploughing at higher speeds, depending upon not only the actual rake angle on contact of the impinging particle and the way (brittle or ductile) the target material respond, but also the greater number of particles that actually come into strike. It is characteristic for an RCE system that a proper turbulent slurry flow condition, relying on the rotation of the specimen shaft, is needed to prevent particle sediment and, thus, to maintain a reasonable wear. In addition to such a wear loss, higher corrosion loss is also expected because of the transport of corrosion species within the EDL is quicker at higher slurry speed.

It is interesting to find that the 304 steel suffering the least weight loss is not the hardest (but the most corrosion resistant) and the 410 steel with the highest hardness suffers greater weight loss than the 304 steel. The least hard and corrosion-resistant mild steel suffers the greatest loss. Such an order of performance is all not consistent with the ranking of mechanical or corrosion properties of the three alloys as expected from Table I. This suggests that corrosion of the 410 steel may have also played an crucial role. It might also be

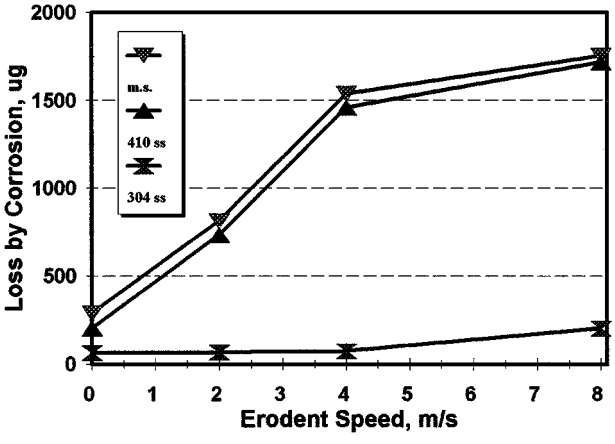

(a)

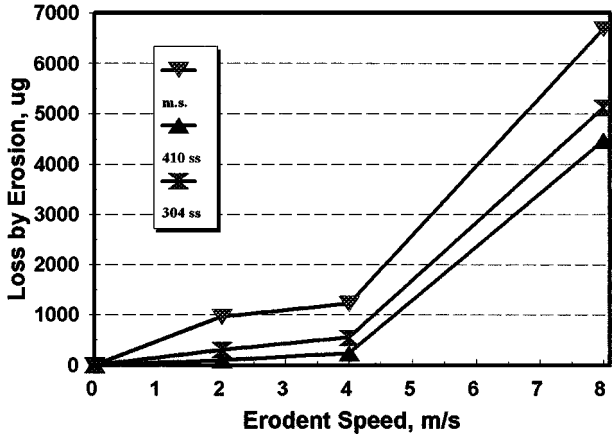

(b)

Figure 8 The weight losses, (a) due to corrosion, (b) due to erosion, of the mild and stainless steels as a function of the slurry speed.

possible that, especially at high slurry speeds, the striking action of the particle have became so intensive that the existing difference of hardness among the materials are overshadowed.

4.3. Surface examinations

Microscopic evidence (Figs 5–7) proves that the surface wear increases with the slurry speed, it shows features of sparsely distributed wear craters for low speeds and highly populated wear scars for high speeds. At 2 m/s, clear cutting scars (due to chipping), and deforming traces (due to ploughing or scratching) are because of the action of angular particles (Fig. 5a and b). Raised material of lips at the exiting rim of a crater with a tail is due to excessive ploughing deformation (Fig. 5b). Material transfer results from the embedding of alumina particles into the mild steel (Fig. 5a). In areas away from the craters, corrosion occurs, this is better seen at higher magnifications (Fig. 5c). In regard to both the stainless steels, features of isolated wear scars are evident (Fig. 5d and f). However, significant corrosion due to either dissolution or pitting occurs to the 410 but not to the 304 steel (compare Fig. 5e and f). The superior corrosion resistance of the austenitic steel is evident. Further, with respect to the morphology and size of the impact craters, discrete differences are found among the three materials. That the crater of the hardest 410 steel is relatively shallow and particles transferred to it is much fewer suggests greater resistance of the martensitic steel to wear (hence a higher erosion resistance). The feather-like pattern at the bottom of craters (Fig. 5d) represents a series of stick-slip movement of the impact particle as it loses kinetic energy in a number of cyclic events of *deforming* the substrate (*stick*) and *switching* to another deforming (*slip*). Such periodic events occur shallower and shallower until the retained kinetic energy become insufficient to deform the target when the particle sweeps away. Similar phenomena are also typical in dry adhesive wear of two hard surfaces, where high friction is a necessity for such a stick-slip to occur [19–22]. High deformation resistance of the 410 steel is thus suggested.

As the slurry speed goes up to 4 m/s (Fig. 6), the surface damage all increases, directly seen from the more densified and uniform surface damages (Fig. 6a, c and f). Two factors are responsible for such a change, one being the greater impact of each individual particle, the other being the greater number of particles impacting on the same surface site. Higher corrosion of the mild steel is identified, in the form of both pits and the grey, porous surface features (Fig. 6b). Similar enhanced corrosion also happens to the 410 steel (Fig. 6e), under the effect of which the aforementioned stick-slip features could only be barely recognisable (Fig. 6d). Contrary to the effect of wear, the effect of corrosion, especially of dissolution, is to smooth the surface. Corrosion thus causes material losses, but also in other ways, such as to assist wear by presenting the corrosion product in a form of vulnerable pits (Fig. 4b and e, for example). As the eroding power increases, the wear difference due to hardness of the three materials is narrowed down. Therefore, typical features of erosive for the 304 (Fig. 6f), the 410 (Fig. 6c) and the mild steel (Fig. 6a) are not significantly different from each other. The corrosion stability of the 304 steel can still be seen (compare Fig. 6f with 6a and c). At further higher speeds (8 m/s, Fig. 7), the effect of hardness differences on particle wear, in terms of wear scar morphology and densities, becomes insignificant between the mild (Fig. 7a and b), the 410 (Fig. 7c and d) and the 304 (Fig. 7e and f) steel. The wear is similarly severe for all the materials (compare the surface ripple-like scars of Fig. 7a, c and e). The corrosion of the mild steel and 410 steel is more severe (Fig. 7b and d), there's however still no convincing severe corrosion of the 304 steel (Fig. 7f, and compare Fig. 7a, c and e). Such evidences proves that the lower, measured weight loss of the relatively soft 304 steel has been resulted from its higher corrosion resistance.

4.4. The separated role of erosion and corrosion

The above surface examinations explains qualitatively from evidence of wear and corrosion the various performances of the materials (Fig. 4). The polarisation curves (Figs 2 and 3) allow insight into the mechanisms of loss from the corrosion point of view. By integrating the corrosion current against time (excluding the cathodic

current values) and using Faraday's second law, the precise weight loss due to corrosion is obtained (Fig. 8a) (the data at zero speed is for pure corrosion), this enables the erosion weight loss to be extracted from Fig. 4 (Fig. 8b). Both the figures quantify the corrosion resistance (Fig. 8a) and the erosion resistance (Fig. 8b) previously analysed. Clearly, the ranking of corrosion resistance and erosion resistance in an ascending order is *mild steel* > 410 *steel* > 304 *steel* and *mild steel* > 304 *steel* > 410 *steel*, respectively. This means the most erosion durable 410 steel is not the most erosion-corrosion resistant one but the less erosion resistant 304 steel is, all because of their higher differences in corrosion resistance (the 304 steel suffers losses ∼1500 μg less at 8 m/s, Fig. 8a) than in erosion resistance (the 410 steel suffers losses ∼500 μg less at 8 m/s, Fig. 8b). In spite of its highest hardness, the overall performance of 410 steel is not the best because of its insufficient resistance to corrosion.

Thus it is the combination of great corrosion resistance and erosion resistance that confers the most desirable erosion-corrosion resistance. However, this should not be misunderstood by underestimating the role of erosion. In fact, in many cases W_e is greater than or approximately equal to W_c (Fig. 8a and b). These are especially the cases of the mild steel (Fig. 9a) and 304 steel (Fig. 9c), in which erosion dominates the erosion-corrosion process. This agrees with conclusions for real production where erosion and corrosion are both present [23, 24]. The situation for the 410 steel at speeds up to 5 m/s (Fig. 9b) shows the vast contrast between its corrosion and erosion properties, thus corrosion as well contributes significantly to the overall material loss.

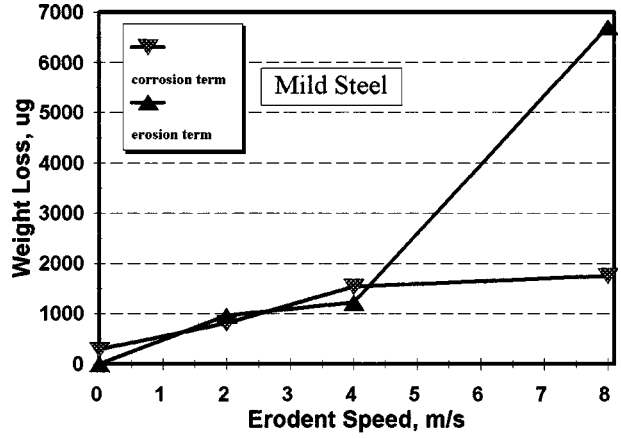

(a)

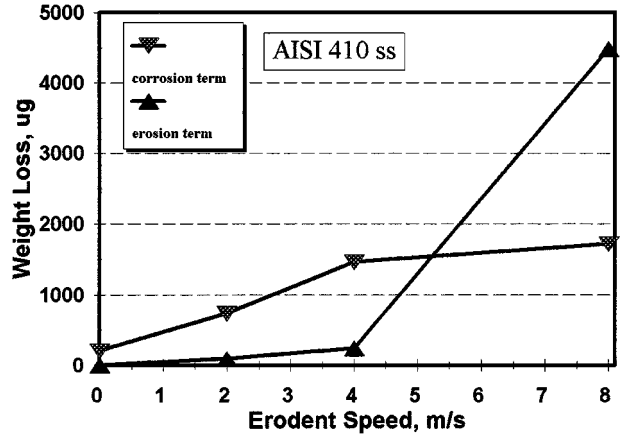

(b)

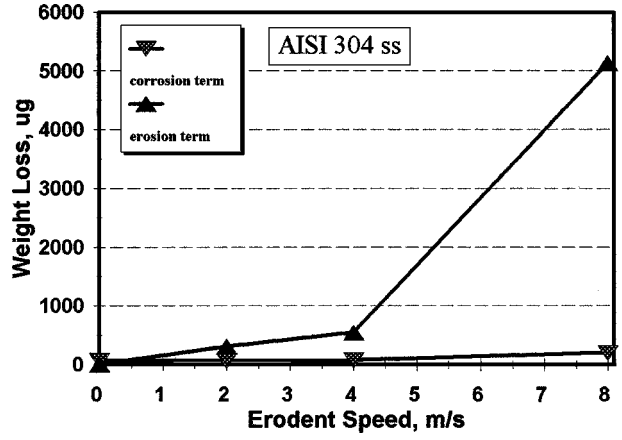

(c)

Figure 9 Comparison of the erosion term and corrosion term, both as a function of the slurry speed for (a) the mild steel, (b) the 410 steel, and (c) the 304 steel.

4.5. Erosion-corrosion mechanisms

The erosion and corrosion in the presence of each other are usually greater than the pure erosion and corrosion, as a result of mutual increasing effect. Erosion enhances corrosion by (1) roughening the surface by formation of fibrous surface textures [25, 26], which intensifies the local electric field and causes higher corrosion at impact crater tops, (2) deforming and introducing stresses to the surface, making it unstable to subsequent electrochemical reactions, and (3) mechanically removing the air-borne oxide or the oxide layer formed by passivation and exposing the fresh metal to corrosion. Such increase may also result due to not only more rapid migration and transport of corroding species (anions and cations) because of mechanical stirring, convection, and thermal current effects [18], but also the "erosion" and destruction of the established EDL which would otherwise, after certain amount of corrosion occurs, reach an equilibrium. Such a dynamic equilibrium, by which the metal ions enter from the substrate into EDL and diffuse away from it into the bulk laminar and turbulent flow zones at an equal rate, and the typical ion concentration profiles are illustrated in Fig. 10. The eventual role of erosion or solution agitation is either to reduce the Me^+ concentration at plane b, C_b, so that corrosion is accelerated, because the Me^+ concentration gradient from *b* to *a* planes represents the resistance of the EDL to substrate dissolution (so-called concentration polarisation controlled), or to reduce laminar flow zone and the diffusion boundary layer thickness [18]. The shortening of the diffusion path eases the transport of corrosive species. These effects can also be expected for corrosion in a flowing solutions free of solid particles, but obviously with less effect.

Corrosion can enhance erosion by making materials more active and unstable. This is because dissolution and gas bubbling both encourages detachment of a premature deformed lip from its crater. The passive film, too thin to be protective, may also assist wear

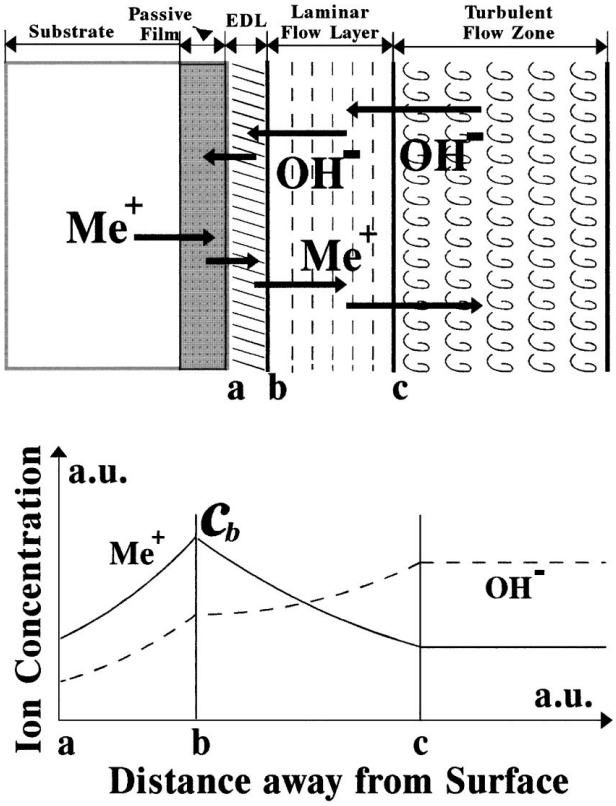

Figure 10 Schematic diagrams showing dissolution corrosion within the electrochemical double layer (EDL) and the typical ion concentration profiles, when an equilibrium is reached, built within the EDL and the bulk flowing solutions (the laminar and turbulent flow zones).

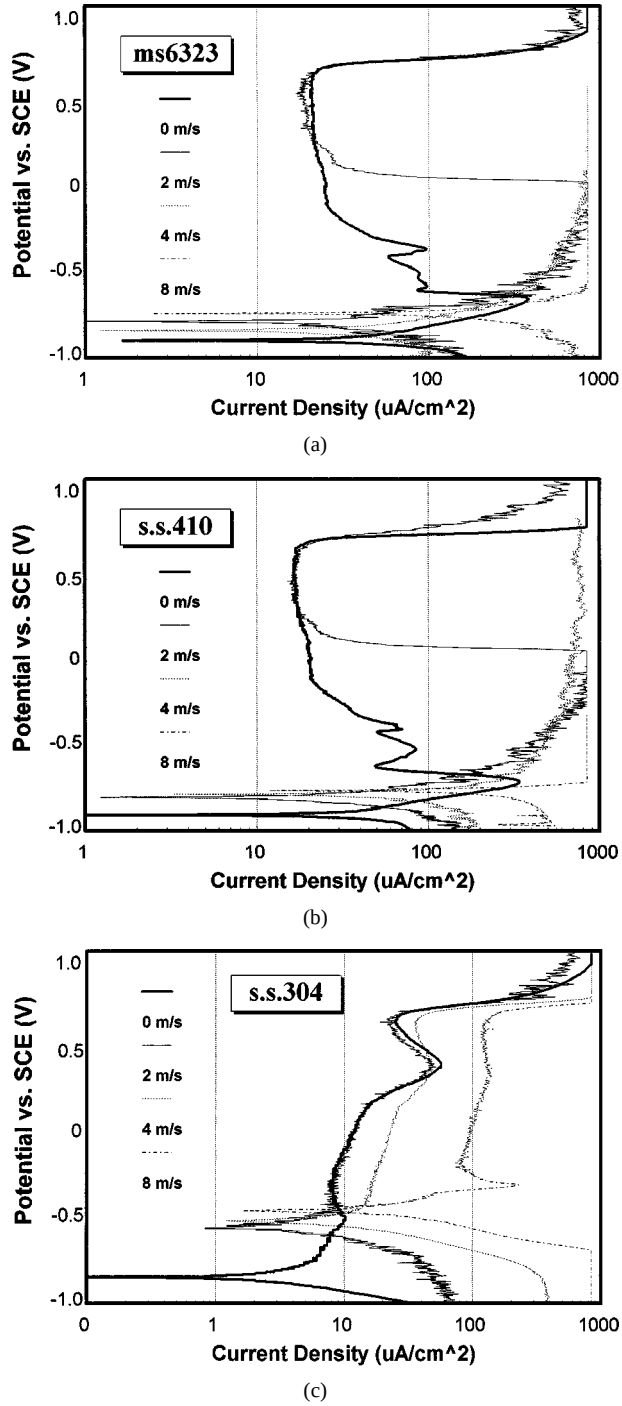

Figure 11 Summary of the polarisation curves of Figs 2 and 3, in terms of performance of each material as a function of the slurry speed, for (a) the mild steel, (b) the 410 steel, and (c) the 304 steel.

debris separation when its adhesion to the substrate is destroyed. Corrosion can further promote erosion by dissolving work-hardened layers and by roughening the surface [25, 26]. The mutual effects of erosion and corrosion are believed to be prominent in the mild steel and 410 steel, because of their high corrosion. Such a result are fundamentally determined by the composition and microstructures involved. For example, the presence of dual phases in the mild steel makes the corrosion non-uniform on the ferrite and cementite phases [27–29]. Such a non-uniform corrosion may also occur to the dual-phase 410 steel.

On basis of the results of Fig. 9, and of Figs 2 and 3 which are summarised in Fig. 11, proposed mechanisms for the erosion-corrosion of the three materials are suggested in Fig. 12. Similar to the erosion-controlled damage in the high temperature erosion [30, 31], the entire erosion-corrosion for all the materials is mainly erosion controlled, but affected by passivation at certain low speeds and by severe dissolution at high speeds for the mild and 410 steel. Distinctly, the erosion for the 304 steel was passivation-affected in the entire speed range. All these processes are passive film penetrative because passive films are too thin. Thus, phenomena, such as oxide scale erosion, or oxide controlled spalling [32–34], associated with thick oxide films at high temperatures, are not found. Hence, erosion of both the passive film, if present, and substrate is proposed in Fig. 12. Fig. 12a and b also illustrate the severe increased dissolution of the mild and 410 steel at high speeds, as compared to that of the 304 steel (Fig. 12c). Such understanding of the erosion-corrosion mechanism and identification of the speed regions within which erosion or corrosion dominates are important because they are a guide for total performance control. Take the 304 steel for instance, since erosion is a major problem (Figs 12c and 9c), strengthening will be a key solution but should be done carefully. In this respect, neither hardening by precipitation of carbides through tempering at the expense of the reduction of the effective amount solid solution of Cr and the corrosion resistance loss, nor strengthening by increase of C, although very effective, with another negative effect of increased sensitisation susceptibility (precipitation of carbides along

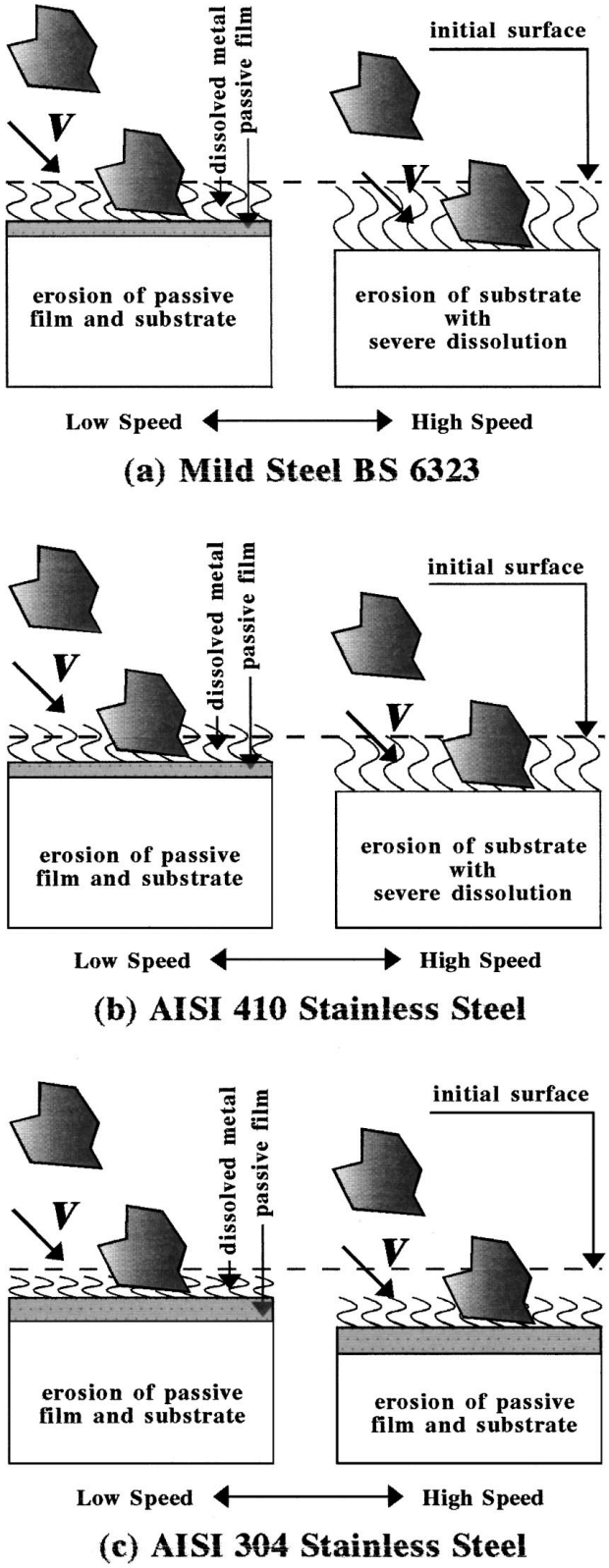

Figure 12 Schematic diagrams illustrating the main mechanisms of the erosion-corrosion process of (a) the mild steel, (b) the 410 steel, and (c) the 304 steel.

austenite grain boundaries, leading to intergranular corrosion) [35], should be used. Since addition of further Cr and Ni to the 304 steel, in the form of solute atoms, can increase both mechanical strength and corrosion resistance [36], steels having compositions similar to those of the AISI 310 or AISI 314 stainless steel are expected to have better performances than the 304 steel.

5. Conclusions

1. The above erosive wear under controlled corrosion in the current test conditions showed that the overall resistance to erosion-corrosion in an ascending order was mild steel, BS6323, the AISI 410 stainless steel, and the AISI 304 stainless steel, the precise difference among them being dependent upon the specific particle velocity regimes. Microscopical evidence showed that the wear damage to them all increased with the particle velocity, and the wear features on the eroded scars were different at low velocities but all became similar at high velocities. Further, evidence of increasing corrosion on the eroded-corroded surface was found for the mild and the stainless 410 steels, but there was no convincing evidence of significant corrosion for the 304 stainless steel.

2. That the medium-hard, AISI 304 stainless steel having higher corrosion resistance (stronger passivity) outperformed the hardest AISI 410 steel having lower corrosion resistance (weaker passivity) suggested that corrosion might play an equally important role with erosion, especially at high particle velocity. At low velocity, the weight loss difference due to different hardness between the 410 and 304 (and the mild) steels was evident, as confirmed by microscopical examination. As the particle velocity increased, the hardness effect was reduced and the corrosion behaviour difference became pronounced. That explained the increased difference between the performance of the 410 and 304 steels at higher velocities.

Acknowledgements

The authors wish to thank the Engineering and Physical Sciences Research Council, UK, for financial support of this project and award of a research associateship to HWW.

References

1. Y. ZHENG, Z. YAO, X. WEI and W. KE, *Wear* **186/187** (1995) 555.
2. R. J. K. WOOD and S. P. HUTTON, *ibid.* **140** (1990) 387.
3. I. M. HUTCHINGS, "Tribology: Friction and Wear of Engineering Materials" (Edward Arnold, London, 1992).
4. I. FINNIE, *Wear* **186/187** (1995) 1.
5. A. W. RUFF and S. M. WIEDERHORN, in "Treatise on Materials Science and Technology," Vol. 16, edited by C. M. Preece (Academic Press, New York, 1979) p. 69.
6. R. BROWN, S. KOSCO and E. J. JUN, *Wear* **88** (1983) 181.
7. I. G. WRIGHT, V. NAGARAJAN and R. B. HERCHENROEDER, in "Corrosion-Erosion Behaviour of Materials," edited by K. Natesan (The Metallurgical Society of AIME., Philadelphia, 1980) p. 268.
8. J. C. SCULLY, "The Fundamentals of Corrosion" 3rd ed. (Pergamon Press, Oxford, 1990).
9. L. P. MYERS, in "Handbook of Stainless Steels," edited by D. Peckner and I. M. Bernstein (McGraw-Hill, New York, 1977) p. 11-1.
10. E. SNAPE, in "Handbook of Stainless Steels," edited by D. Peckner and I. M. Bernstein (McGraw-Hill, New York, 1977) p. 12-1.
11. L. R. SCHARFSTEIN, in "Handbook of Stainless Steels," edited by D. Peckner and I. M. Bernstein (McGraw-Hill, New York, 1977) p. 15-1.
12. H. W. WANG and M. M. STACK, *Surf. Coat. Technol.* **105** (1998) 141.

13. M. M. STACK, H. W. WANG and W. D. MUNZ, *ibid.* **113** (1999) 52.
14. B. WALLEN and J. OLSSON, in "Handbook of Stainless Steels," edited by D. Peckner and I. M. Bernstein (McGraw-Hill, New York, 1977) p. 16–1.
15. M. DROGOWSKA, H. MENARD and L. BROSSARD, *J. Appl. Electrochem.* **26** (1996) 217.
16. *Idem., ibid.* **27** (1997) 169.
17. M. DROGOWSKA, H. MENARD, A. LASIA and L. BROSSARD, *ibid.* **26** (1996) 1169.
18. B. VYAS, in "Treatise on Materials Science and Technology," Vol. 16, edited by C. M. Preece (Academic Press, New York, 1979) p. 357.
19. B. J. LANCE and F. SADEGHI, *J. Tribo-Trans. ASME.* **115** (1993) 445.
20. H. YOSHIZAWA, P. MCGUIGGAN and J. ISRAELACHVILI, *Science* **259** (1993) 1305.
21. S. V. PRASAD and K. R. MECKLENBURG, *Wear* **162** (1993) 47.
22. S. C. TUNG and S. S. WANG, *Tribo. Trans.* **35** (1992) 298.
23. J. POSTOLETHWAITE, E. D. B. TINKER and M. W. HAWRYLAK, *Corro.* **30** (1974) 285.
24. J. POSTOLETHWAITE and D. N. HOLDER, *Can. J. Chem. Eng.* **54** (1976) 255.
25. Y. OKA, H. KOUZAI and M. MATSUMURA, *Corro. Eng.* **35** (1986) 320.
26. Y. OKA and M. UHKUBO, *Corro.* **46** (1990) 687.
27. A. A. ONO, N. ALONSON and A. P. TSCHIPTSCHIN, *ISIJ International* **36** (1996) 813.
28. D. A. MORENO, M. F. L. DEMELE, J. R. IBARS and H. A. VIDELA, *Corro.* **47** (1991) 2.
29. A. JOSHI and D. F. STEIN, *ibid.* **28** (1972) 321.
30. G. SUNDARARAJAN and R. MANISH, *Tribo. International* **30** (1997) 339.
31. G. SUNDARARAJAN, in Proceedings of Corrosion-Erosion-Wear of Materials at Elevated Temperatures, edited by A. V. Levy (National Association of Corrosion Engineers, Texas, 1991) p. 11.
32. A. V. LEVY, E. SLAMOVCH and N. JEE, *Wear* **110** (1986) 117.
33. I. G. WRIGHT, V. NAGARAJAN and J. STRINGER, *Oxid.Met.* **25** (1986) 175.
34. A. V. LEVY and B. WANG, *Surf. Coat. Technol.* **33** (1987) 285.
35. J. J. HEGER and J. L. HAMILTON, *Corro.* **11** (1955) 22.
36. A. J. SEDRIKS, "Corroison of Stainless Steels" (John Wiley & Sons, New York, 1979).

Received 20 January
and accepted 15 March 2000